Search for New Particles Decaying to $t\bar{t}$ in $p\bar{p}$ Collisions at $\sqrt{s} = 1.8$ TeV

T. Affolder,[21] H. Akimoto,[43] A. Akopian,[36] M. G. Albrow,[10] P. Amaral,[7] S. R. Amendolia,[32] D. Amidei,[24] K. Anikeev,[22] J. Antos,[1] G. Apollinari,[36] T. Arisawa,[43] T. Asakawa,[41] W. Ashmanskas,[7] M. Atac,[10] F. Azfar,[29] P. Azzi-Bacchetta,[30] N. Bacchetta,[30] M. W. Bailey,[26] S. Bailey,[14] P. de Barbaro,[35] A. Barbaro-Galtieri,[21] V. E. Barnes,[34] B. A. Barnett,[17] M. Barone,[12] G. Bauer,[22] F. Bedeschi,[32] S. Belforte,[40] G. Bellettini,[32] J. Bellinger,[44] D. Benjamin,[9] J. Bensinger,[4] A. Beretvas,[10] J. P. Berge,[10] J. Berryhill,[7] B. Bevensee,[31] A. Bhatti,[36] M. Binkley,[10] D. Bisello,[30] R. E. Blair,[2] C. Blocker,[4] K. Bloom,[24] B. Blumenfeld,[17] S. R. Blusk,[35] A. Bocci,[32] A. Bodek,[35] W. Bokhari,[31] G. Bolla,[34] Y. Bonushkin,[5] D. Bortoletto,[34] J. Boudreau,[33] A. Brandl,[26] S. van den Brink,[17] C. Bromberg,[25] M. Brozovic,[9] N. Bruner,[26] E. Buckley-Geer,[10] J. Budagov,[8] H. S. Budd,[35] K. Burkett,[14] G. Busetto,[30] A. Byon-Wagner,[10] K. L. Byrum,[2] M. Campbell,[24] W. Carithers,[21] J. Carlson,[24] D. Carlsmith,[44] J. Cassada,[35] A. Castro,[30] D. Cauz,[40] A. Cerri,[32] A. W. Chan,[1] P. S. Chang,[1] P. T. Chang,[1] J. Chapman,[24] C. Chen,[31] Y. C. Chen,[1] M. -T. Cheng,[1] M. Chertok,[38] G. Chiarelli,[32] I. Chirikov-Zorin,[8] G. Chlachidze,[8] F. Chlebana,[10] L. Christofek,[16] M. L. Chu,[1] S. Cihangir,[10] C. I. Ciobanu,[27] A. G. Clark,[13] A. Connolly,[21] J. Conway,[37] J. Cooper,[10] M. Cordelli,[12] J. Cranshaw,[39] D. Cronin-Hennessy,[9] R. Cropp,[23] R. Culbertson,[7] D. Dagenhart,[42] F. DeJongh,[10] S. Dell'Agnello,[12] M. Dell'Orso,[32] R. Demina,[10] L. Demortier,[36] M. Deninno,[3] P. F. Derwent,[10] T. Devlin,[37] J. R. Dittmann,[10] S. Donati,[32] J. Done,[38] T. Dorigo,[14] N. Eddy,[16] K. Einsweiler,[21] J. E. Elias,[10] E. Engels, Jr.,[33] W. Erdmann,[10] D. Errede,[16] S. Errede,[16] Q. Fan,[35] R. G. Feild,[45] C. Ferretti,[32] R. D. Field,[11] I. Fiori,[3] B. Flaugher,[10] G. W. Foster,[10] M. Franklin,[14] J. Freeman,[10] J. Friedman,[22] Y. Fukui,[20] S. Galeotti,[32] M. Gallinaro,[36] T. Gao,[31] M. Garcia-Sciveres,[21] A. F. Garfinkel,[34] P. Gatti,[30] C. Gay,[45] S. Geer,[10] D. W. Gerdes,[24] P. Giannetti,[32] P. Giromini,[12] V. Glagolev,[8] M. Gold,[26] J. Goldstein,[10] A. Gordon,[14] A. T. Goshaw,[9] Y. Gotra,[33] K. Goulianos,[36] C. Green,[34] L. Groer,[37] C. Grosso-Pilcher,[7] M. Guenther,[34] G. Guillian,[24] J. Guimaraes da Costa,[24] R. S. Guo,[1] C. Haber,[21] E. Hafen,[22] S. R. Hahn,[10] C. Hall,[14] T. Handa,[15] R. Handler,[44] W. Hao,[39] F. Happacher,[12] K. Hara,[41] A. D. Hardman,[34] R. M. Harris,[10] F. Hartmann,[18] K. Hatakeyama,[36] J. Hauser,[5] J. Heinrich,[31] A. Heiss,[18] M. Herndon,[17] B. Hinrichsen,[23] K. D. Hoffman,[34] C. Holck,[31] R. Hollebeek,[31] L. Holloway,[16] R. Hughes,[27] J. Huston,[25] J. Huth,[14] H. Ikeda,[41] J. Incandela,[10] G. Introzzi,[32] J. Iwai,[43] Y. Iwata,[15] E. James,[24] H. Jensen,[10] M. Jones,[31] U. Joshi,[10] H. Kambara,[13] T. Kamon,[38] T. Kaneko,[41] K. Karr,[42] H. Kasha,[45] Y. Kato,[28] T. A. Keaffaber,[34] K. Kelley,[22] M. Kelly,[24] R. D. Kennedy,[10] R. Kephart,[10] D. Khazins,[9] T. Kikuchi,[41] M. Kirk,[4] B. J. Kim,[19] D. H. Kim,[19] H. S. Kim,[16] M. J. Kim,[19] S. H. Kim,[41] Y. K. Kim,[21] L. Kirsch,[4] S. Klimenko,[11] P. Koehn,[27] A. Köngeter,[18] K. Kondo,[43] J. Konigsberg,[11] K. Kordas,[23] A. Korn,[22] A. Korytov,[11] E. Kovacs,[2] J. Kroll,[31] M. Kruse,[35] S. E. Kuhlmann,[2] K. Kurino,[15] T. Kuwabara,[41] A. T. Laasanen,[34] N. Lai,[7] S. Lami,[36] S. Lammel,[10] J. I. Lamoureux,[4] M. Lancaster,[21] G. Latino,[32] T. LeCompte,[2] A. M. Lee IV,[9] K. Lee,[39] S. Leone,[32] J. D. Lewis,[10] M. Lindgren,[5] T. M. Liss,[16] J. B. Liu,[35] Y. C. Liu,[1] N. Lockyer,[31] J. Loken,[29] M. Loreti,[30] D. Lucchesi,[30] P. Lukens,[10] S. Lusin,[44] L. Lyons,[29] J. Lys,[21] R. Madrak,[14] K. Maeshima,[10] P. Maksimovic,[14] L. Malferrari,[3] M. Mangano,[32] M. Mariotti,[30] G. Martignon,[30] A. Martin,[45] J. A. J. Matthews,[26] J. Mayer,[23] P. Mazzanti,[3] K. S. McFarland,[35] P. McIntyre,[38] E. McKigney,[31] M. Menguzzato,[30] A. Menzione,[32] C. Mesropian,[36] T. Miao,[10] R. Miller,[25] J. S. Miller,[24] H. Minato,[41] S. Miscetti,[12] M. Mishina,[20] G. Mitselmakher,[11] N. Moggi,[3] E. Moore,[26] R. Moore,[24] Y. Morita,[20] A. Mukherjee,[10] T. Muller,[18] A. Munar,[32] P. Murat,[10] S. Murgia,[25] M. Musy,[40] J. Nachtman,[5] S. Nahn,[45] H. Nakada,[41] T. Nakaya,[7] I. Nakano,[15] C. Nelson,[10] D. Neuberger,[18] C. Newman-Holmes,[10] C.-Y. P. Ngan,[22] P. Nicolaidi,[40] H. Niu,[4] L. Nodulman,[2] A. Nomerotski,[11] S. H. Oh,[9] T. Ohmoto,[15] T. Ohsugi,[15] R. Oishi,[41] T. Okusawa,[28] J. Olsen,[44] C. Pagliarone,[32] F. Palmonari,[32] R. Paoletti,[32] V. Papadimitriou,[39] S. P. Pappas,[45] D. Partos,[4] J. Patrick,[10] G. Pauletta,[40] M. Paulini,[21] C. Paus,[22] L. Pescara,[30] T. J. Phillips,[9] G. Piacentino,[32] K. T. Pitts,[16] R. Plunkett,[10] A. Pompos,[34] L. Pondrom,[44] G. Pope,[33] M. Popovic,[23] F. Prokoshin,[8] J. Proudfoot,[2] F. Ptohos,[12] G. Punzi,[32] K. Ragan,[23] A. Rakitine,[22] D. Reher,[21] A. Reichold,[29] W. Riegler,[14] A. Ribon,[30] F. Rimondi,[3] L. Ristori,[32] W. J. Robertson,[9] A. Robinson,[23] T. Rodrigo,[6] S. Rolli,[42] L. Rosenson,[22] R. Roser,[10] R. Rossin,[30] W. K. Sakumoto,[35] D. Saltzberg,[5] A. Sansoni,[12] L. Santi,[40] H. Sato,[41] P. Savard,[23] P. Schlabach,[10] E. E. Schmidt,[10] M. P. Schmidt,[45] M. Schmitt,[14] L. Scodellaro,[30] A. Scott,[5] A. Scribano,[32] S. Segler,[10] S. Seidel,[26] Y. Seiya,[41] A. Semenov,[8] F. Semeria,[3] T. Shah,[22] M. D. Shapiro,[21] P. F. Shepard,[33] T. Shibayama,[41] M. Shimojima,[41] M. Shochet,[7] J. Siegrist,[21] G. Signorelli,[32] A. Sill,[39] P. Sinervo,[23] P. Singh,[16] A. J. Slaughter,[45] K. Sliwa,[42] C. Smith,[17] F. D. Snider,[10] A. Solodsky,[36] J. Spalding,[10] T. Speer,[13] P. Sphicas,[22] F. Spinella,[32] M. Spiropulu,[14] L. Spiegel,[10] J. Steele,[44] A. Stefanini,[32] J. Strologas,[16] F. Strumia, [13] D. Stuart,[10] K. Sumorok,[22] T. Suzuki,[41] T. Takano,[28] R. Takashima,[15] K. Takikawa,[41] P. Tamburello,[9] M. Tanaka,[41] B. Tannenbaum,[5] W. Taylor,[23] M. Tecchio,[24] P. K. Teng,[1] K. Terashi,[41] S. Tether,[22] D. Theriot,[10] R. Thurman-Keup,[2] P. Tipton,[35] S. Tkaczyk,[10] K. Tollefson,[35] A. Tollestrup,[10] H. Toyoda,[28] W. Trischuk,[23] J. F. de Troconiz,[14] J. Tseng,[22] N. Turini,[32] F. Ukegawa,[41] T. Vaiciulis,[35] J. Valls,[37] S. Vejcik III,[10] G. Velev,[10] R. Vidal,[10] R. Vilar,[6] I. Volobouev,[21] D. Vucinic,[22] R. G. Wagner,[2] R. L. Wagner,[10] J. Wahl,[7]

N. B. Wallace,[37] A. M. Walsh,[37] C. Wang,[9] C. H. Wang,[1] M. J. Wang,[1] T. Watanabe,[41] D. Waters,[29] T. Watts,[37] R. Webb,[38] H. Wenzel,[18] W. C. Wester III,[10] A. B. Wicklund,[2] E. Wicklund,[10] H. H. Williams,[31] P. Wilson,[10] B. L. Winer,[27] D. Winn,[24] S. Wolbers,[10] D. Wolinski,[24] J. Wolinski,[25] S. Wolinski,[24] S. Worm,[26] X. Wu,[13] J. Wyss,[32] A. Yagil,[10] W. Yao,[21] G. P. Yeh,[10] P. Yeh,[1] J. Yoh,[10] C. Yosef,[25] T. Yoshida,[28] I. Yu,[19] S. Yu,[31] A. Zanetti,[40] F. Zetti,[21] and S. Zucchelli[3]

(CDF Collaboration)

[1] *Institute of Physics, Academia Sinica, Taipei, Taiwan 11529, Republic of China*
[2] *Argonne National Laboratory, Argonne, Illinois 60439*
[3] *Istituto Nazionale di Fisica Nucleare, University of Bologna, I-40127 Bologna, Italy*
[4] *Brandeis University, Waltham, Massachusetts 02254*
[5] *University of California at Los Angeles, Los Angeles, California 90024*
[6] *Instituto de Fisica de Cantabria, University of Cantabria, 39005 Santander, Spain*
[7] *Enrico Fermi Institute, University of Chicago, Chicago, Illinois 60637*
[8] *Joint Institute for Nuclear Research, RU-141980 Dubna, Russia*
[9] *Duke University, Durham, North Carolina 27708*
[10] *Fermi National Accelerator Laboratory, Batavia, Illinois 60510*
[11] *University of Florida, Gainesville, Florida 32611*
[12] *Laboratori Nazionali di Frascati, Istituto Nazionale di Fisica Nucleare, I-00044 Frascati, Italy*
[13] *University of Geneva, CH-1211 Geneva 4, Switzerland*
[14] *Harvard University, Cambridge, Massachusetts 02138*
[15] *Hiroshima University, Higashi-Hiroshima 724, Japan*
[16] *University of Illinois, Urbana, Illinois 61801*
[17] *The Johns Hopkins University, Baltimore, Maryland 21218*
[18] *Institut für Experimentelle Kernphysik, Universität Karlsruhe, 76128 Karlsruhe, Germany*
[19] *Korean Hadron Collider Laboratory: Kyungpook National University, Taegu 702-701; Seoul National University, Seoul 151-742; and SungKyunKwan University, Suwon 440-746; Korea*
[20] *High Energy Accelerator Research Organization (KEK), Tsukuba, Ibaraki 305, Japan*
[21] *Ernest Orlando Lawrence Berkeley National Laboratory, Berkeley, California 94720*
[22] *Massachusetts Institute of Technology, Cambridge, Massachusetts 02139*
[23] *Institute of Particle Physics: McGill University, Montreal H3A 2T8; and University of Toronto, Toronto M5S 1A7; Canada*
[24] *University of Michigan, Ann Arbor, Michigan 48109*
[25] *Michigan State University, East Lansing, Michigan 48824*
[26] *University of New Mexico, Albuquerque, New Mexico 87131*
[27] *The Ohio State University, Columbus, Ohio 43210*
[28] *Osaka City University, Osaka 588, Japan*
[29] *University of Oxford, Oxford OX1 3RH, United Kingdom*
[30] *Universita di Padova, Istituto Nazionale di Fisica Nucleare, Sezione di Padova, I-35131 Padova, Italy*
[31] *University of Pennsylvania, Philadelphia, Pennsylvania 19104*
[32] *Istituto Nazionale di Fisica Nucleare, University and Scuola Normale Superiore of Pisa, I-56100 Pisa, Italy*
[33] *University of Pittsburgh, Pittsburgh, Pennsylvania 15260*
[34] *Purdue University, West Lafayette, Indiana 47907*
[35] *University of Rochester, Rochester, New York 14627*
[36] *Rockefeller University, New York, New York 10021*
[37] *Rutgers University, Piscataway, New Jersey 08855*
[38] *Texas A&M University, College Station, Texas 77843*
[39] *Texas Tech University, Lubbock, Texas 79409*
[40] *Istituto Nazionale di Fisica Nucleare, University of Trieste/ Udine, Italy*
[41] *University of Tsukuba, Tsukuba, Ibaraki 305, Japan*
[42] *Tufts University, Medford, Massachusetts 02155*
[43] *Waseda University, Tokyo 169, Japan*
[44] *University of Wisconsin, Madison, Wisconsin 53706*
[45] *Yale University, New Haven, Connecticut 06520*

We use 106 pb^{-1} of data collected with the Collider Detector at Fermilab to search for narrow-width, vector particles decaying to a top and an anti-top quark. Model independent upper limits on the cross section for narrow, vector resonances decaying to $t\bar{t}$ are presented. At the 95% confidence level, we exclude the existence of a leptophobic Z' boson in a model of topcolor-assisted technicolor

with mass $M_{Z'} < 480$ GeV/c^2 for natural width $\Gamma = 0.012\ M_{Z'}$, and $M_{Z'} < 780$ GeV/c^2 for $\Gamma = 0.04\ M_{Z'}$.

PACS numbers: 14.65.Ha, 13.85.Ni, 13.85.Qk

In this letter, we present a model-independent search for narrow, vector resonances decaying to $t\bar{t}$. This search is sensitive to, for example, a Z' predicted by topcolor-assisted technicolor [1,2]. This model anticipates that the explanation of spontaneous electroweak symmetry breaking is related to the observed fermion masses, and that the large value of the top quark mass suggests the introduction of new strong dynamics into the standard model. It accounts for the large top quark mass by predicting the existence of a residual global symmetry SU(3)×U(1) at energies below 1 TeV. The SU(3) results in the generation of topgluons which we have searched for previously in the $b\bar{b}$ channel [3]. The U(1) gives the Z' we search for here. In one model [2], the Z' decays exclusively to quarks (leptophobic) resulting in a large cross section for $t\bar{t}$.

With the z-axis defined along the proton beam, the Collider Detector at Fermilab (CDF) coordinate system defines ϕ as the azimuthal angle in the transverse plane, θ as the polar angle, and pseudorapidity η as $-\ln(\tan\frac{\theta}{2})$. Tracking chambers, immersed in a 1.4-Tesla solenoidal magnetic field, are used for the detection of charged particles and the measurement of their momenta. The precision track reconstruction of the silicon microstrip vertex detector (SVX), located immediately outside the beampipe, is used for the detection of displaced secondary vertices resulting from b-quark decays. Outside the SVX is the vertex time projection chamber (VTX) which provides further tracking information for $|\eta| \leq 3.25$. Both the SVX and VTX are housed within the central tracking chamber (CTC), a wire drift chamber used to measure charged particle momenta. Electromagnetic and hadronic calorimeters, located beyond the CTC and superconducting solenoid, measure energy in segmented η-ϕ towers out to $|\eta| < 4.2$. Drift chambers used for muon detection reside outside the calorimetry. A more detailed description of the CDF detector can be found elsewhere [4,5].

Standard model $t\bar{t}$ production in $p\bar{p}$ collisions at a center of mass energy of $\sqrt{s} = 1.8$ TeV is dominated by $q\bar{q}$ annihilation, while ∼10% is attributable to gluon-gluon fusion. Once a $t\bar{t}$ pair is produced, each of the top quarks is expected to decay almost exclusively to Wb. The search presented here focuses on the $t\bar{t}$ event topology in which one W boson decays hadronically while the other decays to an electron or muon and its corresponding neutrino. The fragmentation of the b-quarks, as well as the hadronic daughters of the W boson, form jets. Accordingly, $t\bar{t}$ candidates in this "lepton + jets" channel are characterized by a single lepton, missing transverse energy, $\not\!\!E_T$ [6], due to the undetected neutrino, and at least four jets. Furthermore, a jet resulting from a b-quark can be identified (or "tagged") as such by the reconstruction of a secondary vertex from the b hadron decay using the SVX, or by using the soft lepton tagging (SLT) algorithm to find an additional lepton from a semileptonic b decay [5,7].

Like the top quark mass measurement [8], events included in our measurement of the $t\bar{t}$ invariant mass spectrum must first contain a lepton candidate in the central detector region ($|\eta| < 1.0$). This lepton is required to be either an isolated electron with transverse energy (E_T) in excess of 20 GeV or an isolated muon with transverse momentum (P_T) in excess of 20 GeV/c. Events must also include at least 20 GeV of $\not\!\!E_T$, attributable to the presence of a neutrino, as well as at least four jets with $|\eta| < 2.0$ and raw $E_T > 15$ GeV. Raw jet energies are the values which result from clustering signals in the calorimeter towers before any offline jet corrections are applied. To increase the acceptance rate for $t\bar{t}$ events, the requirements for the fourth jet are relaxed such that the raw E_T must only be greater than 8 GeV with $|\eta| < 2.4$ in events where at least one of the leading three jets is tagged by the SVX or SLT algorithms. All jets in this analysis are formed as clusters of calorimeter towers within cones of fixed radius $\Delta R \equiv \sqrt{(\Delta\eta)^2 + (\Delta\phi)^2} = 0.4$. In 106 pb^{-1} of data, we observe 83 events which satisfy these requirements.

This method builds upon the techniques developed for the top quark mass measurement [8] by fitting each event to the hypothesis of $t\bar{t}$ production followed by decay in the lepton+jets channel:

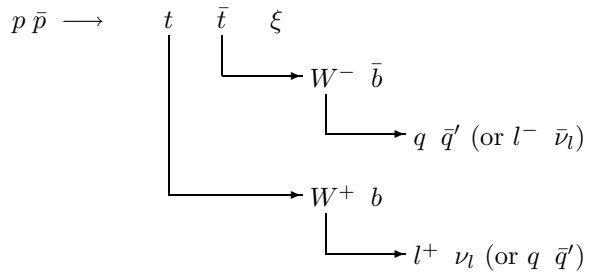

The four-momenta of these 13 objects fully describe a $t\bar{t}$ event. The three-momenta of the charged lepton and four jets are measured directly. To compute the energies of these objects, the b and $\bar{b}$ quark masses are taken to be 5 GeV/c^2, the q and $\bar{q}'$ masses are taken to be 0.5 GeV/c^2, and the charged lepton mass is assigned according to its identification as either an electron or a muon. The components of transverse momentum for the recoiling system, ξ, are measured directly from extra jets in the event and unclustered energy deposits that are not included in lepton or jet energies. The transverse momentum components of the neutrino are computed by requiring that the total E_T in the event sums to zero. While the neutrino is assumed to be massless, its longitudinal momentum is a free parameter in the kinematic fit in which the $q\bar{q}'$ and $\ell\nu$ invariant masses are constrained to equal the W boson mass. We perform a kinematic fit to the production and decay of the $t\bar{t}$ pair as described by the decay chain shown above. This fitting procedure, which depends on the minimization of a χ^2 expression [9], allows the lepton energy, the jet energies and the unclustered energy to vary within their respective uncertainties. The fitted results for these values determine the t and $\bar{t}$

four-momentum, from which the $t\bar{t}$ invariant mass ($M_{t\bar{t}}$) can be computed. To improve the $M_{t\bar{t}}$ resolution, we also constrain the two Wb invariant masses to 175 GeV/c^2, in agreement with the most recent measurement of the top quark mass [10]. We use only the four highest E_T jets, leading to 12 combinations for assigning jets to the b, $\bar{b}$, and hadronic W daughters. However, because we measure only the transverse component of the total energy, thereby determining $\not\!\!E_T$, a two-fold ambiguity in the longitudinal component of the neutrino momentum results in 24 combinations. We further require that jets that are SVX or SLT-tagged be assigned to b-quarks, thereby reducing the number of combinations.

Electron energies and muon momenta are measured with the calorimeter and tracking chambers, respectively [11]. A set of generic jet corrections is applied to the energies of all the jets in an event to account for absolute energy scale calibration, contributions from the underlying event and multiple interactions, as well as energy losses in cracks between detector components and outside the clustering cone. These corrections are determined from a combination of Monte Carlo simulations and data [12]. The four leading jets in a $t\bar{t}$ event undergo an additional energy correction that depends on the type of parton that they are assumed to be in the fit: a light quark, a hadronically decaying b quark, or a b quark that decayed semileptonically. These parton-specific corrections account for (a) the differences in the expected P_T distributions of jets from $t\bar{t}$ and the shape which was assumed to derive the generic jet corrections mentioned above, and (b) the energy losses from semileptonic b and c-hadron decays. These corrections were derived from a study of $t\bar{t}$ events generated with the HERWIG Monte Carlo program [13].

Using Monte Carlo simulations of signal and background events, we explored several event selection criteria in an attempt to optimize our discovery potential [14]. Of the 24 possibilities for each event, we select the $M_{t\bar{t}}$ value which corresponds to the configuration with the lowest χ^2. To reduce the probability of selecting configurations with incorrect parton assignments which tend to yield artificially low values of $M_{t\bar{t}}$, we refit each event after releasing the constraint that the Wb invariant mass be equal to 175 GeV/c^2 and demand that the fit for this particular configuration return a value for the top quark mass between 150 GeV/c^2 and 200 GeV/c^2. To further reduce incorrect combinations and to increase discovery potential for a new particle decaying to $t\bar{t}$, we apply a χ^2 cut. For narrow width $t\bar{t}$ resonances, simulation predicts that the width of the $M_{t\bar{t}}$ spectrum is $\sim 6\%$ of the resonance mass for cases in which the correct jet configuration is selected. For resonances with a natural width Γ that is significantly less than 6% of the nominal mass, the CDF detector resolution will dominate and the resonances will all have approximately the same shape (shown in the inset of Fig. 1 for a mass of 500 GeV/c^2). At low $M_{t\bar{t}}$, the presence of residual events with incorrect parton assignments is evident in this figure.

The selection criteria described above eliminate an additional 20 events from our data sample and the resulting $M_{t\bar{t}}$ spectrum is shown in Fig. 1, along with the expected standard model $t\bar{t}$ and QCD W+jets background shapes normalized to the data. While the non-$t\bar{t}$ background is dominated by W+jets events, it also includes contributions from multijet $b\bar{b}$ events with one jet misidentified as a lepton, Z+jets events, events with a boson pair, and single-top production. However, it has been shown that the VECBOS [15] W+jets shape alone is sufficient in modeling the entire non-$t\bar{t}$ background spectrum [8]. For this analysis, the expected non-$t\bar{t}$ background prediction of 31.1 $\pm$ 8.5 events is calculated as in Ref. [9], but accounts for differences in selection criteria. We find that the $M_{t\bar{t}}$ distribution of 63 data events is consistent with the hypothesis that the spectrum is comprised of standard model $t\bar{t}$ production and the predicted rate of non-$t\bar{t}$ background events, as shown in Fig. 1.

Because we cannot present evidence for a narrow $t\bar{t}$ resonance, we establish upper limits on the production cross-section for a new vector particle, X, of mass M_X decaying and to $t\bar{t}$. For natural widths $\Gamma = 0.012M_X$ and $\Gamma = 0.04M_X$, and for each M_X between 400 GeV/c^2 and 1 TeV/c^2 in increments of 50 GeV/c^2, we perform a binned-likelihood fit of the data. To determine the likelihood function for a given M_X and Γ, we fit the $M_{t\bar{t}}$ spectrum from the data to the expected Monte Carlo shapes for both the $t\bar{t}$ and QCD W+jets background sources as well as a resonance signal $X \rightarrow t\bar{t}$ which we model using $Z' \rightarrow t\bar{t}$ in PYTHIA [16].

Our analysis is subject to several sources of systematic uncertainty on the expected shape of background and signal $M_{t\bar{t}}$ spectra and/or the signal acceptance rate. Treating these two types of systematic effect separately, we establish the magnitude of each source through a Monte Carlo procedure which quantifies the effect of varying the source of uncertainty by one standard deviation. We determine the uncertainty contributions due to the jet E_T scale, initial and final state gluon radiation, and the non-$t\bar{t}$ background spectrum using methods described in Ref. [9]. The uncertainty in the measurements of the top quark mass [10] and total integrated luminosity [17] are included in our study of systematic effects, as well as the uncertainty due to the choice of parton distribution functions (PDF). The remaining sources of systematic uncertainty considered are all small and include trigger efficiency, lepton identification, tracking efficiency, z-vertex efficiency, and Monte Carlo statistics. The uncertainties resulting from jet E_T scale and top quark mass are correlated and we conservatively take this correlation to be 100%.

The percent uncertainty in $\sigma_X \cdot \mathrm{BR}\{X \rightarrow t\bar{t}\}$ is listed in Table I for each of the systematic sources at several different resonance masses. The systematic effect due to uncertainty in the top quark mass (M_{top}) is dominant at low M_X, whereas the effect due to the uncertainty in modeling final state radiation dominates at large M_X. To ensure that our estimates are conservative, the sys-

tematic uncertainty is taken to be a constant number of pb below the value of $\sigma_{\rm X} \cdot {\rm BR}\{{\rm X} \to t\bar{t}\}$ corresponding to the 95% C.L. limit obtained with statistical uncertainties only [14]. That constant is the estimate of the systematic uncertainty at the 95% C.L. limit. Above the same value of $\sigma_{\rm X} \cdot {\rm BR}\{{\rm X} \to t\bar{t}\}$, we use a systematic uncertainty that rises with $\sigma_{\rm X} \cdot {\rm BR}\{{\rm X} \to t\bar{t}\}$ at the fixed percent rate listed in Table I.

For each resonance mass and width, we convolute the statistical likelihood shape with the Gaussian total systematic uncertainty and extract the 95% C.L. upper limit on $\sigma_{\rm X} \cdot {\rm BR}\{{\rm X} \to t\bar{t}\}$ which is listed in Table II and shown in Fig. 2. The systematic uncertainties increase the 95% C.L. upper limit by 27% for $M_{\rm X} = 400$ GeV/c^2, but only 7% (6%) for $M_{\rm X} = 600$ (800) GeV/c^2 because statistical uncertainties dominate the likelihood. Also shown in Fig. 2 are the theoretical predictions for cross-section times branching ratio for a leptophobic Z' with natural width $\Gamma = 0.012 M_{Z'}$ and $\Gamma = 0.04 M_{Z'}$ [2]. At 95% confidence, we exclude the existence of a leptophobic topcolor Z' with mass $M_{Z'} < 480$ GeV/c^2 for natural width $\Gamma = 0.012\ M_{Z'}$, and mass $M_{Z'} < 780$ GeV/c^2 for $\Gamma = 0.04\ M_{Z'}$. For larger widths, detector resolution will no longer be the dominant factor in determining the Z' signal shape, so our limits are no longer applicable.

In conclusion, after investigating 106 pb^{-1} of data collected at CDF, we find no evidence for a $t\bar{t}$ resonance and establish upper limits on cross-section times branching ratio for narrow resonances. We have used these limits to constrain a model of topcolor assisted technicolor.
We thank the Fermilab staff and the technical staffs of the participating institutions for their vital contributions. This work is supported by the U.S. Department of Energy and the National Science Foundation; the Natural Sciences and Engineering Research Council of Canada; the Istituto Nazionale di Fisica Nucleare of Italy; the Ministry of Education, Science and Culture of Japan; the National Science Council of the Republic of China; and the A.P. Sloan Foundation.

[1] C. T. Hill, Phys. Lett. B **345**, 483 (1995); C. T. Hill and S. J. Parke, Phys. Rev. D **49**, 4454 (1994).
[2] R. M. Harris, C. T. Hill, and S. J. Parke, Fermilab-FN-687, hep-ph/9911288 (1999).
[3] F. Abe *et al.*, Phys. Rev. Lett. **82**, 2038 (1999).
[4] F. Abe *et al.*, Nucl. Instrum. Methods, A **271**, 387 (1988).
[5] F. Abe *et al.*, Phys. Rev. D **50**, 2966 (1994).
[6] The transverse momentum of a particle is $\mathrm{P_T} = P sin\theta$. The analogous quantity using calorimeter energies, defined as $\mathrm{E_T} = E sin\theta$, is called transverse energy. Missing transverse energy $\not\!\!\mathrm{E}_{\rm T}$ is defined as $-\sum \mathrm{E}^i_{\rm T}\, \hat{n}_i$, where $\hat{n}_i$ are the unit vectors pointing from the interaction point to the energy deposition in the calorimeter.
[7] F. Abe *et al.*, Phys. Rev. Lett. **74**, 2626 (1995).
[8] F. Abe *et al.*, Phys. Rev. Lett. **80**, 2767 (1998).
[9] T. Affolder *et al.*, "Measurement of the Top Quark Mass using the Collider Detector at Fermilab," (to be submitted to Phys. Rev. D).
[10] L. Demortier, R. Hall, R. Hughes, B. Klima, R. Roser, M. Strovink, Fermilab Preprint Fermilab-TM-2084.
[11] F. Abe *et al.*, Phys. Rev. D **52**, 4784 (1995).
[12] F. Abe *et al.*, Phys. Rev. D **47**, 4857 (1993).
[13] G. Marchesini and B.R. Webber, Nucl. Phys. B **310**, 461 (1988); G. Marchesini *et al.*, Comput. Phys. Commun. **67**, 465 (1992). We use HERWIG version 5.6.
[14] J. Cassada, Ph.D. Thesis, University of Rochester, 1999 (unpublished).
[15] F.A. Berends, W.T. Giele, H. Kuijf, and B. Tausk, Nucl. Phys. B **357**, 32 (1991).
[16] T. Sjöstrand, Comput. Phys. Commun. **82**, 74 (1994). We use PYTHIA version 5.7.
[17] D. Cronin-Hennessy, A. Beretvas, P.F. Derwent, (to be published in Nucl. Instrum. Methods Phys. Res. Sect. A).

$M_{\rm X}$ (GeV/c^2) / Source	400	600	800
Jet $\mathrm{E_T}$	6.1	6.2	4.4
M_{top}	22	3.1	8.7
Jet $\mathrm{E_T}$ and M_{top}	28	9.3	13
Initial state radiation	14	4.2	5.6
Final state radiation	19	16	12
b-tagging bias	4.6	0.79	0.85
PDF	11	5.5	4.8
QCD background shape	1.3	0.17	0.045
Additional acceptance effects	5.3	5.3	5.3
Luminosity	4.0	4.0	4.0
Total	39	21	20

TABLE I. The percent systematic uncertainty in $\sigma_{\rm X} \cdot {\rm BR}\{{\rm X} \to t\bar{t}\}$ from various sources.

$M_{\rm X}$ ($\rm GeV/c^2$)	95% C.L. upper limit $\sigma_{\rm X} \cdot {\rm BR}\{{\rm X} \to t\bar{t}\}$ (pb)	
	for $\Gamma = 0.012 M_{\rm X}$	for $\Gamma = 0.04 M_{\rm X}$
400	6.60	6.51
450	5.21	6.32
500	7.31	6.97
550	3.58	3.95
600	1.92	2.23
650	1.82	1.92
700	1.53	1.63
750	1.21	1.27
800	0.97	1.07
850	0.91	1.02
900	0.93	1.08
950	1.00	1.10
1000	1.00	1.23

TABLE II. The 95% C.L. upper limit on the cross section times branching ratio for vector particles decaying to $t\bar{t}$, as a function of mass, for two natural widths.

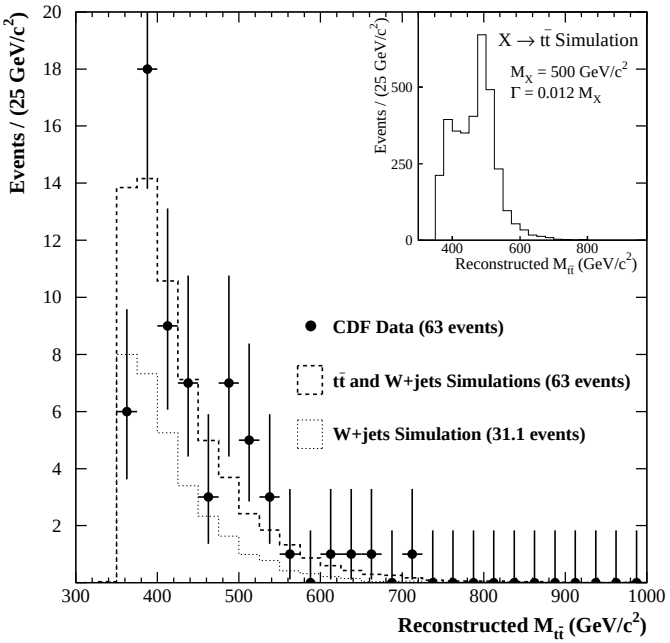

FIG. 1. The observed $M_{t\bar{t}}$ spectrum (points) compared to the QCD W+jets background (fine dashes) and the total standard model prediction including both QCD W+jets and $t\bar{t}$ production (thick dashes). The $t\bar{t}$ prediction has been normalized such that the number of events in the total standard model prediction is equal to the number of events in the data. The inset shows the expected $M_{t\bar{t}}$ shape resulting from the simulation of a narrow, vector $X \to t\bar{t}$ resonance ($M_{\rm X} = 500$ GeV/c^2, $\Gamma = 0.012 M_{\rm X}$) in the CDF detector.

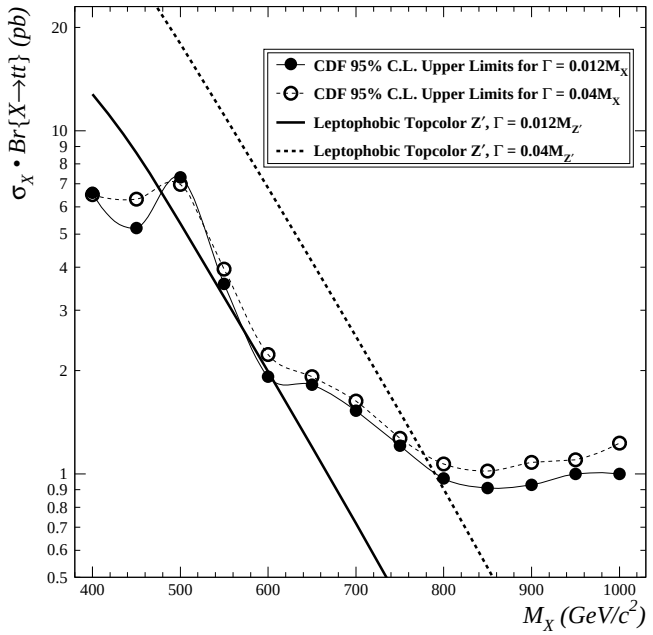

FIG. 2. The 95% C.L. upper limits on $\sigma_{\rm X} \cdot {\rm BR}\{{\rm X} \to t\bar{t}\}$ as a function of mass (solid and open points) compared to the cross section for a leptophobic topcolor Z' (thick solid and dashed curves) for two resonance widths ($\Gamma = 0.012\ M_{Z'}$ and $\Gamma = 0.04\ M_{Z'}$).